RESEARCH PAPER

$MnCo_2O_4/Co_3O_4$ Nanocomposites: Microwave-Assisted Synthesis, Characterization and Photocatalytic Performance

***Indah Raya** [1], **Gunawan Widjaja** [2], **Kadda Hachem** [3], **Rodin M.N.** [4], **Ahmed A. Ali** [5*], **Mustafa M. Kadhim** [6], **Yasser Fakri Mustafa** [7], **Zaid Hameed Mahmood** [8], **Surendar Aravindhan** [9]*

[1] *Departement of Chemistry,Faculty Mathematics and Natural Science, Hasanuddin University, Makassar,South Sulawesi, Indonesia*

[2] *Faculty of Public Health, Universitas Indonesia, Indonesia*

[3] *Department of biology, Faculty of sciences, University of Saida - Dr. Moulay Tahar, Algeria*

[4] *Sechenov First Moscow State Medical University, Moscow, 119991, Russian Federation*

[5] *College of Petroleum Engineering, Al-Ayen University, Thi-Qar, Iraq*

[6] *Dentistry Department, Kut University College, Kut, Wasit, Iraq*

[7] *Department of Pharmaceutical Chemistry, College of Pharmacy, University of Mosul, Mosul, Iraq*

[8] *Chemistry department, college of science , Diyala university, Iraq*

[9] *Department of Pharmacology, Saveetha dental College and hospital, Saveetha institute of medical and technical sciences, Chennai, India*

ARTICLE INFO

Article History:
Received 23 July 2021
Accepted 09 September 2021
Published 01 October 2021

Keywords:
Microwave
$MnCo_2O_4/Co_3O_4$
Nanocomposites
Photocatalysis

ABSTRACT

In this research, $MnCo_2O_4/Co_3O_4$ nanocomposites were prepared via simple and fast microwave method. The effect of irradiation power and irradiation type (continuous and non-continuous irradiation) on crystalline structure, purity, size and morphological properties of products were investigated via X-ray diffraction (XRD) analysis, energy dispersive spectroscopy (EDS), Transmission Electron Microscopy (TEM), FT-IR and Scanning Electron Microscopy (SEM) respectively. Results revealed that shape and morphological properties of $MnCo_2O_4/Co_3O_4$ nanocomposites can be affected via power and time of microwave irradiation. In the next step, prepared nanocomposites were applied for photodegradation of rhodamine B and methyl violet as organic pollutants. Findings demonstrated that $MnCo_2O_4/Co_3O_4$ nanocomposites can degrade rhodamine B and methyl violet via 58% and 61% efficiency.

How to cite this article
Raya I, Widjaja G, Kadda Hachem et al.. $MnCo_2O_4/Co_3O_4$ Nanocomposites: Microwave-Assisted Synthesis, Characterization and Photocatalytic Performance. J Nanostruct, 2021; 11(4):728-735. DOI: 10.22052/JNS.2021.04.010

INTRODUCTION

Transition-metal oxides based nanocomposites exhibit novel properties that significantly have different physical and chemical properties than those matrix material and the filler resulting [1-4]. In other hand, nanocomposites have a unique and attractive properties due to small size effect [5, 6]. Magnetic nanocomposites not only have unique size-dependent properties but also get benefits from interesting magnetic properties. The magnetic nanocomposites due to vast variety of different materials have high capability in different

* *Corresponding Author Email: ahmed.ali@alayen.edu.iq*

application fields, ranging from biomedical to photocatalysis applications [7-9]. Photocatalysis is a type of catalysis that speeding up the rate of a photoreaction - a chemical reaction that involves the absorption of light by one or more reacting species - by adding catalysts that participate in the chemical reaction without being consumed [10, 11]. A photocatalyst is defined as a material that is capable of absorbs Ultraviolet (UV) radiation from sunlight or illuminated, producing electron–hole pairs that enable chemical transformations of the reaction participants and regenerate its chemical composition after each cycle of such interactions. An efficient photocatalyst should benefits desirable optical features, suitable morphological properties and reusability [12-14].

Cobalt oxide (Co_3O_4) is an important magnetic and P-type semiconductor. Till now, wide range of Co_3O_4 based nanocomposites have been prepared and applied in photocatalysis field [12, 15, 16]. Yong sheng Yan and et al. prepared carbon modified Co_3O_4/BiVO4 p-n heterojunction photocatalyst (Co_3O_4/BiVO4/C) for enhancing light absorption and the facilitating separation of photogenerated charge carriers through forming a p-n heterojunction. They reported that optimum activity of the $Co_3O_4/BiVO_4/C$ p-n heterojunction is higher than that of pure Co_3O_4 and $BiVO_4$ for the degradation of tetracycline under visible light [17]. In other work, Xinfa Dong and et al. prepared $Co_3O_4/Cd_{0.9}Zn_{0.1}$ nanocmposites via solvothermal method. Under visible light, they showed $Co_3O_4/Cd_{0.9}Zn_{0.1}$ H_2 evolution is 15.88 times higher than that obtained over the bare $Cd_{0.9}Zn_{0.1}S$ [18]. Ashok Kumar Chakraborty synthesized Co_3O_4/WO_3 nanocomposites by dispersing p-type semiconductor Co_3O_4 on the surface of n-type semiconductor WO_3. Results revealed that prepared nanocomposites have higher photocatalytic activity than WO_3, Co_3O_4 nanoparticles for the complete decomposition of 2-propanol in gas phase and phenol in aqueous phase and evolution of CO_2 under visible light irradiation [19].

In this work, $MnCo_2O_4/Co_3O_4$ nanocomposites were prepared via simple and low-cost microwave-assisted method. The as-prepared products were characterized by different analyses such as XRD, SEM, TEM, FT-IR, and UV-Vis and the photocatalytic performance of the product was investigated by degradation percent of methylene blue as an organic pollutant under UV irradiation.

MATERIALS AND METHOD

$Co(CH_3COO)_2.4H_2O$ and of $Mn(CH_3COO)_2.4H_2O$ and ethylene glycol was purchased from Merck and all the chemicals were used as received without further purifications. XRD patterns were recorded by a Philips, X-ray diffractometer using Ni-filtered CuKα radiation. Fourier transform infrared (FTIR) spectra were detected by means of Nicolet Magna-550 spectrometer in KBr pellets. The UV–Vis diffuse reflectance analysis of the as-prepared nanocomposite was done by applying a UV–vis spectrophotometer (Shimadzu, UV-2550, Japan). SEM images were obtained using a TESCAN instrument model Mira3 to taking images, the samples were coated by a very thin layer of Pt to make the sample surface conductor and prevent charge accumulation, and obtaining a better contrast. Transmission electron microscopy (TEM) image was achieved via a Philips EM208 transmission electron microscope with an accelerating voltage of 200 kV.

Synthesis $MnCo_2O_4/Co_3O_4$ nanocomposite

$Co(CH_3COO)_2.4H_2O$ and of $Mn(CH_3COO)_2.4H_2O$ with 1:1 molar ratio were dissolved in water/ethylene glycol solvent, which was mixed with a ratio of 2:1. After completely dissolving, the gained transparent solution was transferred to the microwave oven and placed under irradiation at various time and power. The obtained precipitate was washed with distilled water and dry at 85 °C for 5h. Eventually, the product was calcined at 600 °C for 3h. Three samples were prepared at 10 minutes irradiation with power of 900 and 750.

Photocatalytic test

For photocatalyst testing, the amount of 0.05 g of nanocomposites is added to a dye with10 ppm concentration in the quartz reactor. Then the mixture was placed in photoreactor after stirred for 30 min at dark, the UV light was applied. Then $MnCo_2O_4/Co_3O_4$ nanocomposites was separated from the 5 ml samples, taken from the degraded solution at various time intervals, using 5 min centrifuging at 12,000 rpm. The dye concentration was determined with aid of a UV-vis spectrophotometer. The test was performed for 120 minutes.

RESULTS AND DISCUSSION

XRD analysis, which is the most useful and functional technique for both existence and

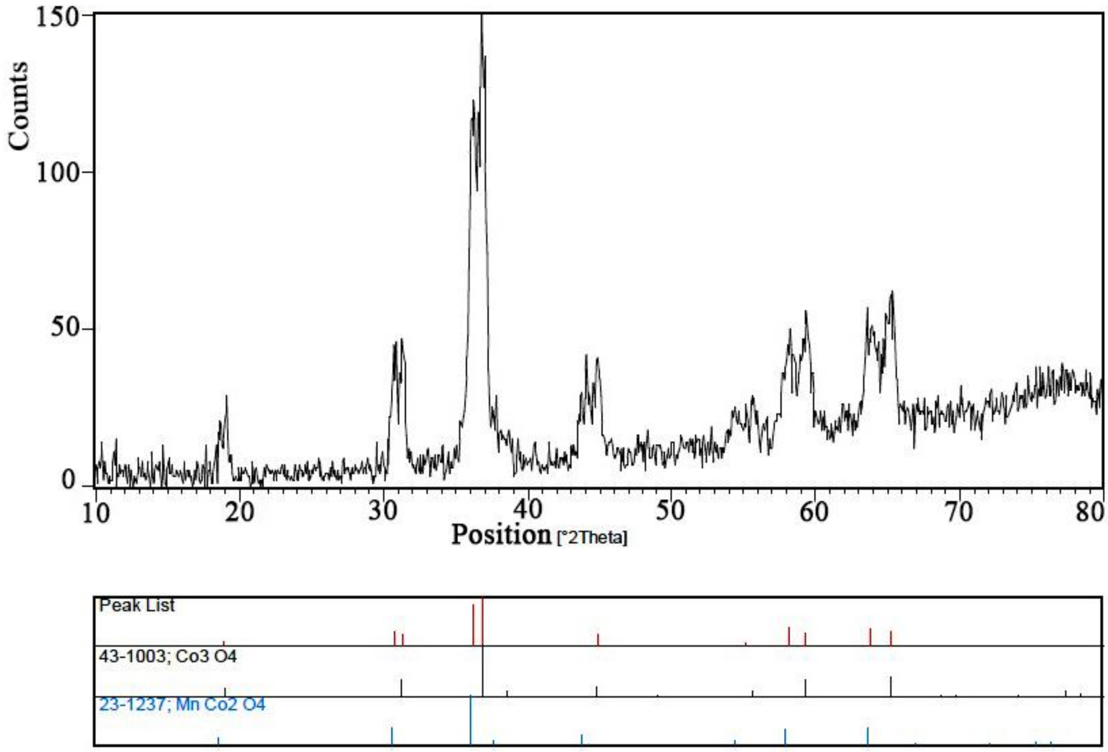

Fig. 1. XRD pattern of $MnCo_2O_4$/ Co_3O_4 Nanocomposites prepared at 10 min in 900 W.

identification of crystalline structure, was hired to investigate the synthesized samples. Fig. 1 shows XRD pattern of $MnCo_2O_4$/ Co_3O_4 nanocomposites. It can be observed Cubic phase of Co_3O_4 (JCPDS: 43-1003) with space group of Fd3m and cell constants a = b = c = 8.0840 Å and Cubic phase of $MnCo_2O_4$ (JCPDS: 23-1237) with space group of Fd3m and cell constants a = b = c = 8.2690 Å were formed. The crystalline size was calculated from Scherrer equation, $Dc = K\lambda/\beta Cos\theta$, where β is the width of the observed diffraction peak at its half maximum intensity (FWHM), K is the shape factor, which takes a value of about 0.9, and λ is the X-ray wavelength (CuKα radiation, equals to 0.154 nm) was about 19 nm.

Fourier transform infrared (FT-IR) spectroscopy has been employed for analysis of the surface functional groups of $MnCo_2O_4$/ Co_3O_4 nanocomposites at 10 min in 900 W after calcination at 600 °C for 3h. As shown in Fig. 2, the most prominent absorption bands at 657 cm-1 and 560 cm^{-1} are corresponding to metal-oxygen bonds in spinel structure of composite [20]. Due to the calcination of the sample at 600 ° C, no further peaks were observed in the sample. Furthermore, the broad bands observed at 3436 cm^{-1} were attributed to the OH groups stretching vibrations of the water molecules [21].

The elemental composition analysis of the as-synthesized $MnCo_2O_4$/ Co_3O_4 nanocomposites at 10 min in 900 W were further confirmed by EDS analysis. As can be seen in Fig. 3, the $MnCo_2O_4$/ Co_3O_4 nanocomposites were composed of stoichiometric Co, Mn and O elements, which indicating the high purity of the products. This result is consistent with the results of XRD pattern presented in Fig. 1.

To investigate the effect of the power and type of irradiation on the morphology and particle size of the $MnCo_2O_4$/ Co_3O_4 nanocomposites the samples were fabricated by using the power of 900 and 750 W for 10 min, and 900 W with cyclic reaction (1 min on and 30 sec off). To assess the effect of these conditions SEM images were investigated. As can be seen in Fig. 4, when the power is set to (a) 750 W, larger particles are formed due to the moderate radiation power. At (b) 900 W, Due to the high radiation power, the ratio of nucleation to growth speeds up, resulting in smaller particles. Also in (c) cyclic reaction, when radiation is present, nucleation occurs and the particles are formed but when radiation is cut off, the particles

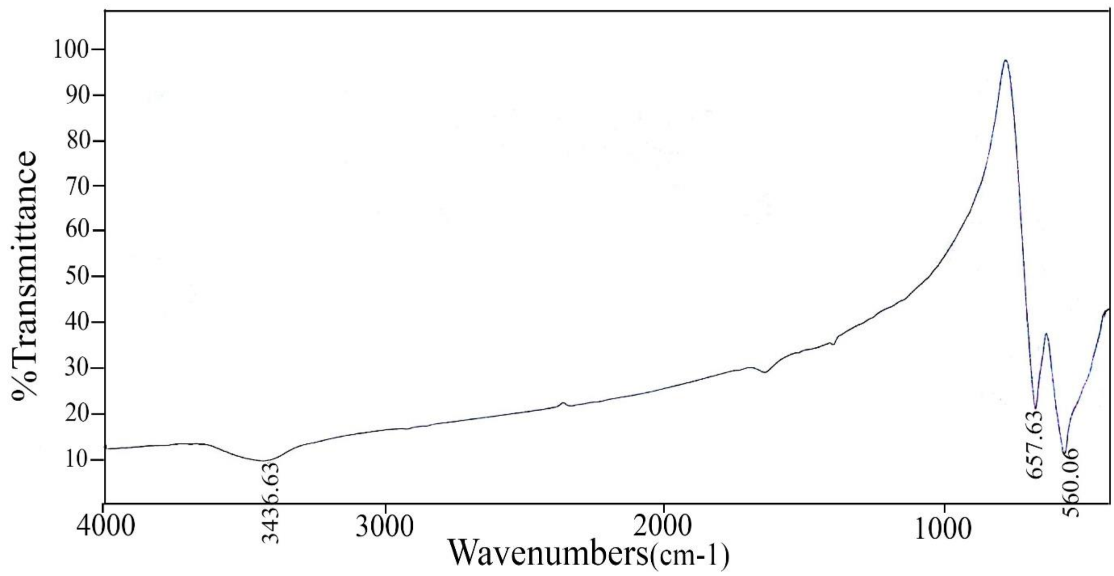

Fig. 2. FT-IR spectrum of $MnCo_2O_4$/ Co_3O_4 Nanocomposites prepared at 10 min in 900 W.

of opportunity grow, resulting in larger particles. According to SEM images, the sample obtained at 900 W and 10 min was selected as the optimum sample.

TEM analysis was applied to in-depth investigation of size and morphological properties of $MnCo_2O_4$/ Co_3O_4 nanocomposites. It is worth bearing in mind that SEM analysis cannot distinguish between Co_3O_4 and $MnCo_2O_4$ in $MnCo_2O_4$/ Co_3O_4 nanocomposites. Fig. 5 illustrated TEM images in different magnification validate uniform nanoparticles of as-prepared

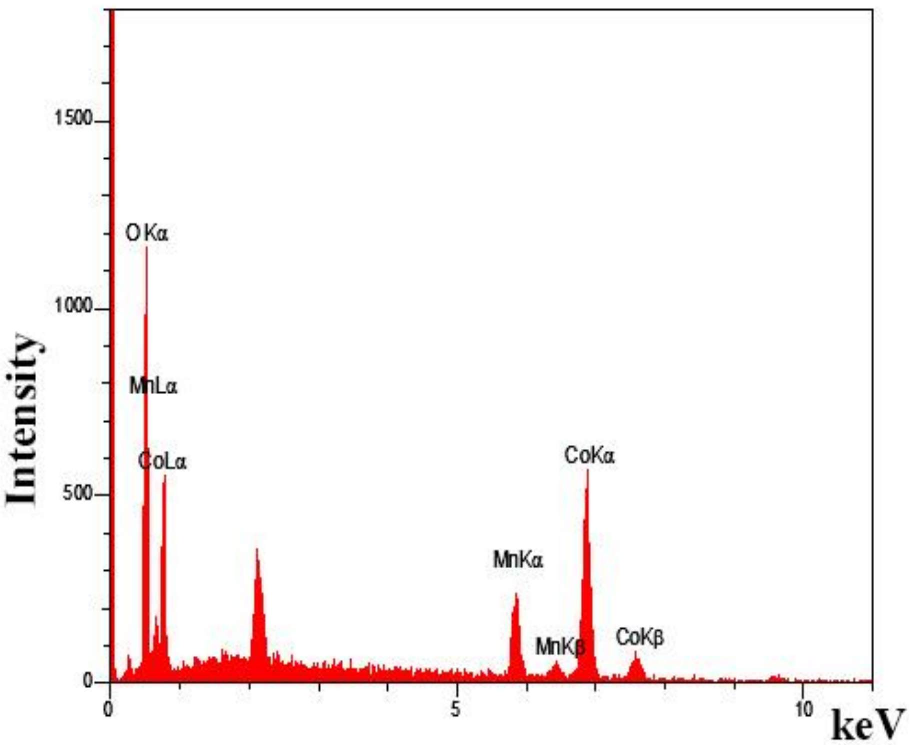

Fig. 3. EDS spectrum of $MnCo_2O_4$/ Co_3O_4 Nanocomposites prepared at 10 min in 900 W.

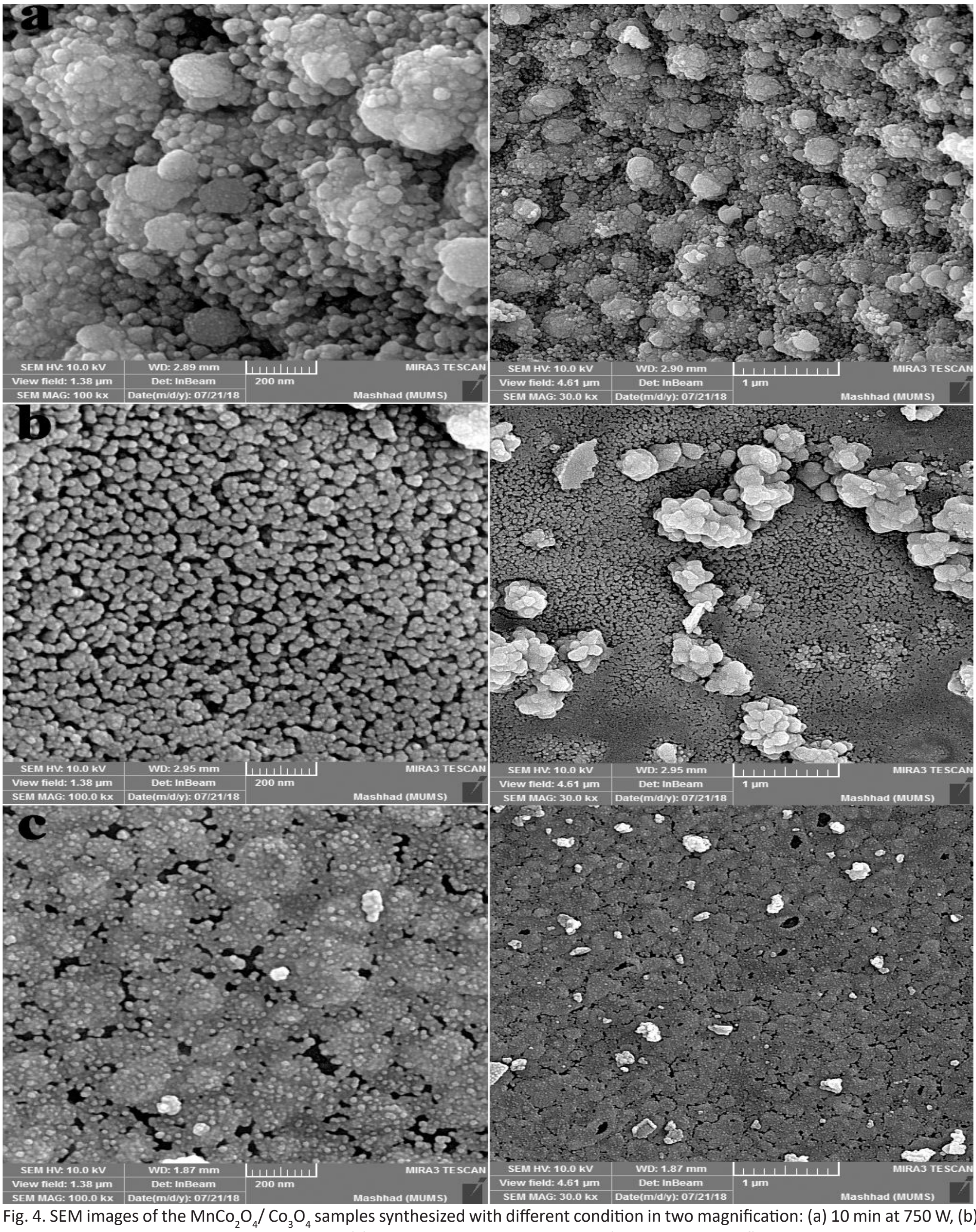

Fig. 4. SEM images of the $MnCo_2O_4$/ Co_3O_4 samples synthesized with different condition in two magnification: (a) 10 min at 750 W, (b) 10 min at 900 W, (c) 10 min at 900 W cyclic reaction (1min on 30 sec off).

nanocomposites via 35 nm in diameter.

Fig. 6 presents the UV-Vis diffuse reflectance spectra (DRS) of the as-prepared $MnCo_2O_4$/ Co_3O_4 nanocomposites (samples). It can be observed that the nanocomposites have strong and broad absorption peaks in the range of 250-400 nm. The value of energy band gap (Eg) of the corresponding nanoparticles is calculated 3.3 eV,

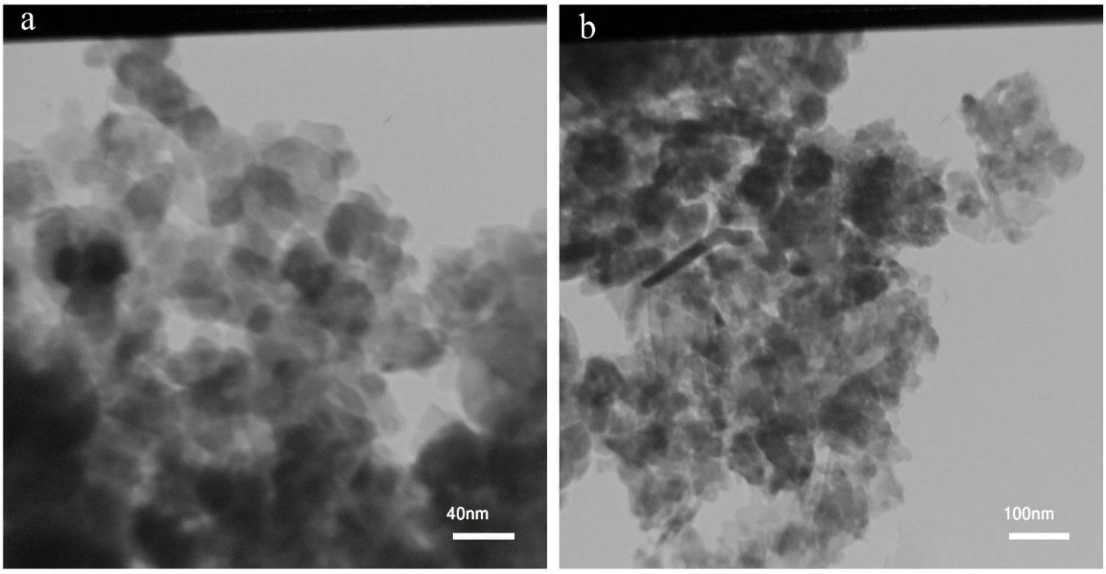

Fig. 5. TEM images of the $MnCo_2O_4$/ Co_3O_4 Nanocomposites prepared at 10 min in 900 W

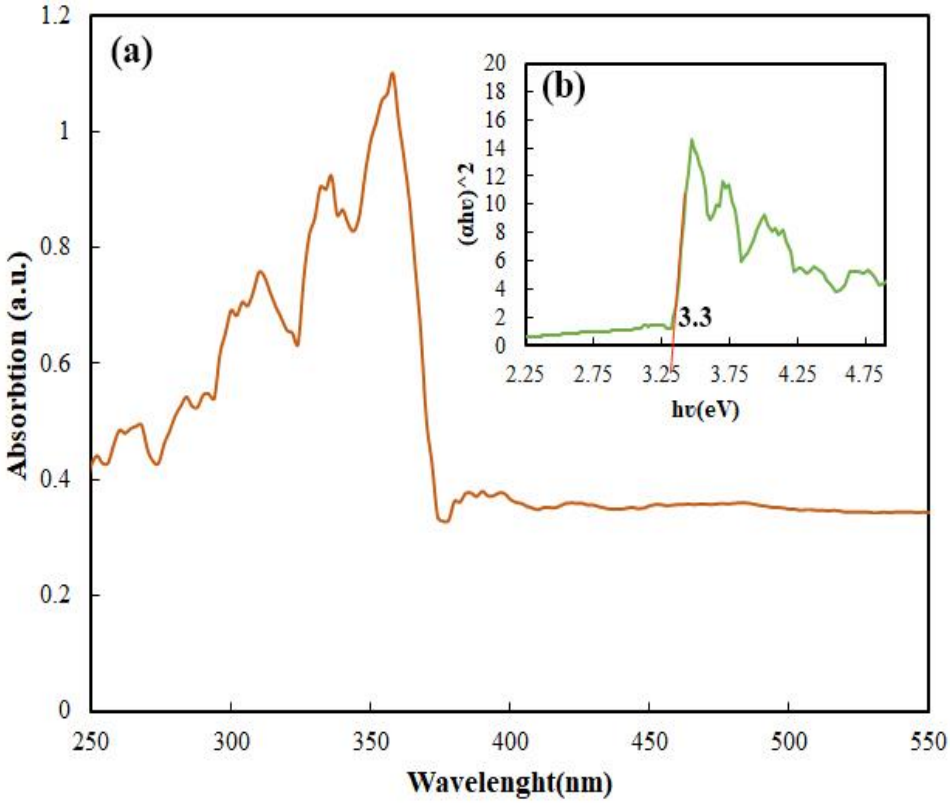

Fig. 6. (a) UV-Vis diffuse reflectance spectrum (DRS) of the $MnCo_2O_4$/ Co_3O_4 Nanocomposites prepared at 10 min in 900 W, and (b) the plot of $(\alpha h\upsilon)^2$ against $h\upsilon$ to determine the band gaps.

based on Tauc's equation[22], which indicating the nanocomposites can be employed as a potential photocatalyst for degradation water soluble dye as a pollution.

Optical properties of product implies that prepared nanocomposites can be applied

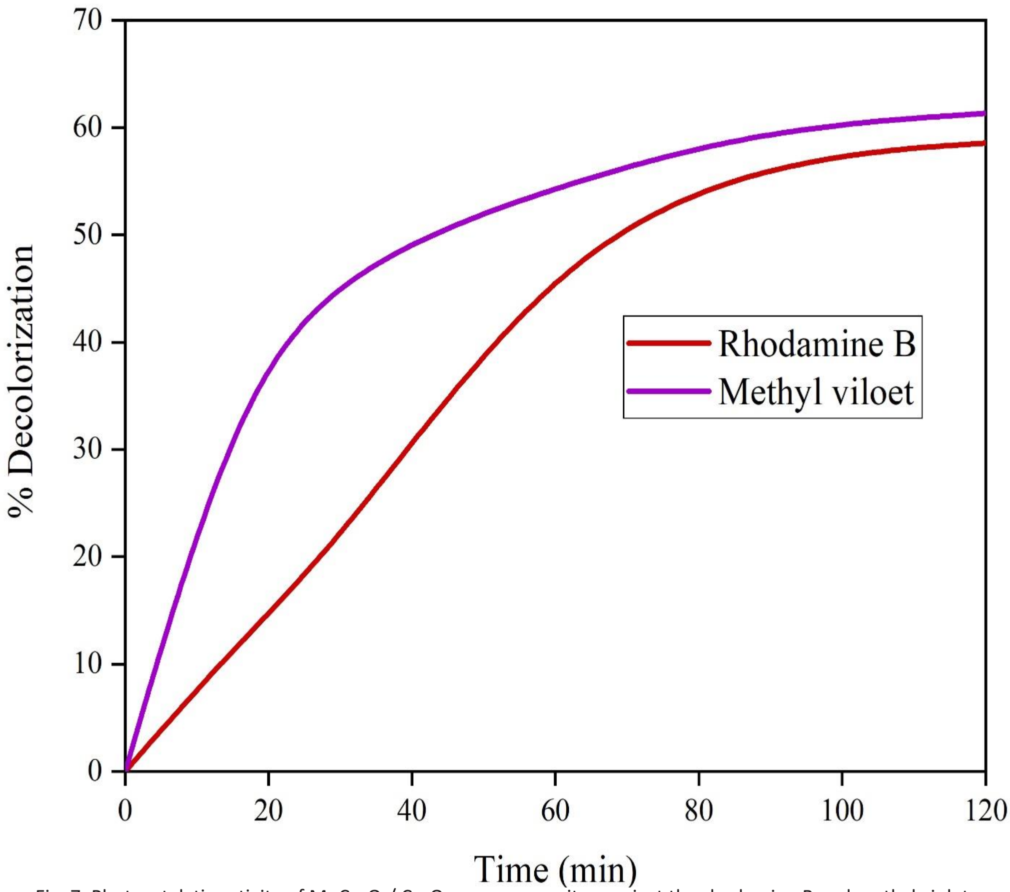

Fig. 7. Photocatalytic activity of $MnCo_2O_4$/ Co_3O_4 nanocomposites against the rhodamine B and methyl violet

in photocatalytic process. Rhodamine B and methyl violet are selected as organic pollutants for investigation of photocatalytic efficiency of $MnCo_2O_4$/ Co_3O_4 nanocomposites under UV irradiation. Results are presented in Fig. 7. For methyl violet case, it can be seen that dye is degraded very faster in early 30 min irradiation. After 30 min, degradation rate was gone down gradually. It can be related to occupying active sites on the $MnCo_2O_4$/ Co_3O_4 nanocomposites (adsorption route). After 120 min, approximately 61% of methyl violet was degraded. For rhodamine B, degradation rate keeps constant after 80 min. After 120 min, approximately 58% of rhodamine B was degraded under UV irradiation. The electronic band structure of prepared $MnCo_2O_4$/ Co_3O_4 nanocomposites make it very good candidate for photocatalytic degradation. As well as mentioned in Fig. 6, the band gap of prepared nanocomposites was calculated 3.3 eV. This means that under UV irradiation, electrons can be moved from valance band to conducting bond in $MnCo_2O_4$/ Co_3O_4 nanocomposites. This movement can be lead to generation of holes (h^+). Photogenerated holes can convert water to hydroxide ions (OH^-). OH^- reacts with h^+ and produce hydroxyl radical ($OH^•$). Produced $OH^•$ could give rise to oxidation of dyes [24].

$$h\upsilon \rightarrow e^- + h^+ \quad (1)$$

$$h^+ + H_2O \rightarrow H^+ + OH^- \quad (2)$$

$$h^+ + OH^- \rightarrow OH^• \quad (3)$$

$$OH^• + dye \rightarrow \text{Oxidation dye} \quad (4)$$

In the parallel pathway, photogenerated OH^- in reaction (2) can be reacted with dissolved oxygen and produce ozone (O_3). Produced ozone can be converted to $O_3^•$ through reaction with photogenerated electron in conducting bond. Generated $O_3^•$ could be degraded dye.

$$2\,OH^- + O_2 + 2h^+ \rightarrow O_3 + H_2O \quad (5)$$

$$e^- + O_3 \rightarrow O_3^• \quad (6)$$

$O_3^{\bullet}$+ dye → Oxidation dye (7)

CONCLUSION

In conclusion, microwave-assisted route was applied for preparation of $MnCo_2O_4/Co_3O_4$ nanocomposites. Prepared products were characterized via XRD, FT-IR, EDS, SEM and TEM analysis. Optical properties of products was investigated via UV-Vis spectroscopy. Results cleared that prepared $MnCo_2O_4/Co_3O_4$ nanocomposites are good candidate for photocatlytic processs. Fot this purpose, $MnCo_2O_4/Co_3O_4$ nanocomposites were applied for photodegradation of rhodamine B and methyl violet. Findings showed that rhodamine B and methyl violet were degraded via 58% and 61% efficiency.

CONFLICT OF INTEREST

The authors declare that there are no conflicts of interest regarding the publication of this manuscript.

REFERENCES

1. Guo X, Zhang G, Li Q, Xue H, Pang H. Non-noble metal-transition metal oxide materials for electrochemical energy storage. Energy Storage Materials. 2018;15:171-201.
2. Goswami C, Hazarika KK, Bharali P. Transition metal oxide nanocatalysts for oxygen reduction reaction. Materials Science for Energy Technologies. 2018;1(2):117-128.
3. Raveau B, Caignaert V, Hardy V, Seikh MM. Transition metal oxides with triangular metallic sublattices: From multiferroics to low-dimensional magnets. Comptes Rendus Chimie. 2018;21(10):952-957.
4. Luches P. Ultrathin Transition Metal Oxide Films. In: Wandelt K, editor. Encyclopedia of Interfacial Chemistry. Oxford: Elsevier; 2018. p. 388-397.
5. Serenko OA, Roldughin VI, Askadskii AA, Serkova ES, Strashnov PV, Shifrina ZB. The effect of size and concentration of nanoparticles on the glass transition temperature of polymer nanocomposites. RSC Advances. 2017;7(79):50113-50120.
6. Yoon KH, Park SB, Yang BD. Size effect of nanoparticles on the conjugated polymer in PPV/SiO_2 nanocomposites. Materials Chemistry and Physics. 2004;87(1):39-43.
7. Burke NAD, Stöver HDH, Dawson FP. Magnetic Nanocomposites: Preparation and Characterization of Polymer-Coated Iron Nanoparticles. Chemistry of Materials. 2002;14(11):4752-4761.
8. Soto GD, Meiorin C, Actis DG, Mendoza Zélis P, Moscoso Londoño O, Muraca D, et al. Magnetic nanocomposites based on shape memory polyurethanes. European Polymer Journal. 2018;109:8-15.
9. Zhuang Y, Zhang X, Chen Q, Li S, Cao H, Huang Y. Co_3O_4/CuO hollow nanocage hybrids with high oxidase-like activity for biosensing of dopamine. Materials Science and Engineering: C. 2019;94:858-866.
10. Yahya N, Aziz F, Jamaludin NA, A. Mutalib M, Ismail AF, W. Salleh WN, et al. A review of integrated photocatalyst adsorbents for wastewater treatment. Journal of Environmental Chemical Engineering. 2018.
11. Hassanpour M, Safardoust-Hojaghan H, Salavati-Niasari M. Rapid and eco-friendly synthesis of NiO/ZnO nanocomposite and its application in decolorization of dye. Journal of Materials Science: Materials in Electronics. 2017;28(15):10830-10837.
12. Liu N, Li Z. Bimetal-organic frameworks derived carbon doped ZnO/Co_3O_4 heterojunction as visible-light stabilized photocatalysts. Materials Science in Semiconductor Processing. 2018;79:24-31.
13. Zhang Y, Jin Z, Yuan H, Wang G, Ma B. Well-regulated nickel nanoparticles functional modified ZIF-67 (Co) derived Co_3O_4/CdS p-n heterojunction for efficient photocatalytic hydrogen evolution. Applied Surface Science. 2018;462:213-225.
14. Zheng J, Lei Z. Incorporation of CoO nanoparticles in 3D marigold flower-like hierarchical architecture $MnCo_2O_4$ for highly boosting solar light photo-oxidation and reduction ability. Applied Catalysis B: Environmental. 2018;237:1-8.
15. Hassanpour M, Safardoust-Hojaghan H, Salavati-Niasari M. Degradation of methylene blue and Rhodamine B as water pollutants via green synthesized Co_3O_4/ZnO nanocomposite. Journal of Molecular Liquids. 2017;229:293-299.
16. Zhang H, Tian W, Guo X, Zhou L, Sun H, Tadé MO, et al. Flower-like Cobalt Hydroxide/Oxide on Graphitic Carbon Nitride for Visible-Light-Driven Water Oxidation. ACS Applied Materials & Interfaces. 2016;8(51):35203-35212.
17. Zhao X, Lu Z, Ma W, Zhang M, Ji R, Yi C, et al. One-step fabrication of carbon decorated $Co_3O_4/BiVO_4$ p-n heterostructure for enhanced visible-light photocatalytic properties. Chemical Physics Letters. 2018;706:440-447.
18. Han Y, Liang Z, Dang H, Dong X. Extremely high photocatalytic H2 evolution of novel $Co_3O_4/Cd_{0.9}Zn_{0.1}S$ p–n heterojunction photocatalyst under visible light irradiation. Journal of the Taiwan Institute of Chemical Engineers. 2018;87:196-203.
19. Chakraborty AK, Shanjeda Akter M, Ahsanul Haque M, Arifuzzaman Khan GM, Shamsul Alam M. Synthesis of Co_3O_4/WO_3 Nanoheterojunction Photocatalyst for the Decomposition of Organic Pollutants Under Visible Light Irradiation. Journal of Cluster Science. 2013;24(3):701-713.
20. Antunović V, Ilić M, Baošić R, Jelić D, Lolić A. Synthesis of $MnCo_2O_4$ nanoparticles as modifiers for simultaneous determination of Pb (II) and Cd (II). PloS one. 2019;14(2):e0210904.
21. Sangsefidi FS, Salavati-Niasari M. Thermal decomposition synthesis, characterization and electrochemical hydrogen storage characteristics of $Co_3O_4–CeO_2$ porous nanocomposite. International Journal of Hydrogen Energy. 2017;42(31):20071-20081.
22. Tauc J, Grigorovici R, Vancu A. Optical Properties and Electronic Structure of Amorphous Germanium. physica status solidi (b). 1966;15(2):627-637.